*Plant Physiology*, September 1999, Vol. 121, pp. 253–261, www.plantphysiol.org © 1999 American Society of Plant Physiologists

# Sulfate Is Both a Substrate and an Activator of the Voltage-Dependent Anion Channel of Arabidopsis Hypocotyl Cells[1]

**Jean-Marie Frachisse*, Sébastien Thomine[2], Jean Colcombet, Jean Guern, and Hélène Barbier-Brygoo**

Institut des Sciences Végétales, Centre National de la Recherche Scientifique, Unité Propre de Recherche 40, Avenue de la Terrasse, 91198 Gif sur Yvette cedex, France

**On the basis of the anion content of in vitro-cultured Arabidopsis plantlets, we explored the selectivity of the voltage-dependent anion channel of the plasma membrane of hypocotyl cells. In the whole-cell configuration, substitution of cytosolic $Cl^-$ by different anions led to the following sequence of relative permeabilities: $NO_3^-$ (2.6) ≥ $SO_4^{2-}$ (2.0) > $Cl^-$ (1.0) > $HCO_3^-$ (0.8) ≫ malate$^{2-}$ (0.03). Large whole-cell currents were measured for $NO_3^-$ and $SO_4^{2-}$, about five to six times higher than the equivalent $Cl^-$ currents. Since $SO_4^{2-}$ is usually considered to be a weakly permeant or non-permeant ion, the components of the large whole-cell current were explored in more detail. Aside from its permeation through the channel with a unitary conductance, about two-thirds that of $Cl^-$, $SO_4^{2-}$ had a regulatory effect on channel activity by preventing the run-down of the anion current both in the whole-cell and the outside-out configuration, increasing markedly the whole-cell current. The fact that the voltage-dependent plasma membrane anion channel of hypocotyl cells can mediate large $NO_3^-$ and $SO_4^{2-}$ currents and is regulated by nucleotides favors the idea that this anion channel can contribute to the cellular homeostasis of important metabolized anions.**

Plant anion channels play central roles in signal transduction and cell turgor regulation. They have been implicated in stomatal function, where their activation is thought to be one of the limiting steps in the loss of guard cell turgor leading to stomatal closure (for review, see Ward et al., 1995). Pharmacological arguments in favor of the involvement of anion channels in elicitor signal transduction have been obtained in cultured parsley and soybean cells (Ebel and Cosio, 1994; Jabs et al., 1997). Recent studies in Arabidopsis hypocotyls have also shown that anion channel activation might be a step in the transduction of two signals modulating hypocotyl growth: blue light (Cho and Spalding, 1996) and auxin (Thomine et al., 1997b). Although anion channels are implicated in a wide range of physiological functions in plant cells, their detailed characterization is still far from complete in differentiated cells other than stomatal guard cells.

The determination of ions that permeate a channel is important, as it may be indicative of its specific physiological role. In particular, the ability of a given channel to transport a particular anion species suggests that this channel could be involved not only in the general processes of membrane depolarization and cell turgor decrease but also, more specifically, in the regulation of the concentration of this anion. For some anions such as $NO_3^-$, which are substrates for intracellular metabolic enzymes, this type of regulation might be important to maintain a suitable intracellular concentration. In parallel with patch-clamp studies of animal systems, the properties of most plant anion channels have been explored with $Cl^-$ as the permeating anion, in spite of the fact that $Cl^-$ is rarely accumulated in plant cells at high concentrations. Anions other than $Cl^-$ could be more relevant substrates for plant anion channels, but only in a few cases has the selectivity of anion channels been extensively studied (Hedrich and Marten, 1993; Elzenga and VanVolkenburgh, 1994; Schmidt and Schroeder, 1994; Skerrett and Tyerman, 1994).

Previous studies of anion channels residing at the plasma membrane in the hypocotyl epidermal cells of Arabidopsis allowed us to characterize a voltage-dependent anion channel (Thomine et al., 1995). This channel is tightly controlled by the transmembrane voltage, being deactivated at resting membrane potentials and activated by depolarization. In a detailed study, we recently showed that voltage regulation is under the control of cytoplasmic nucleotides and does not require nucleotide hydrolysis (Thomine et al., 1997a). A pharmacological characterization of the channel has revealed a poor sensitivity to most anion channel blockers except niflumic acid (Thomine et al., 1997a). We explored the selectivity of this channel toward physiological anions, which has not been previously investigated to our knowledge. Analysis of the anion content of in vitro-grown Arabidopsis plantlets showed that $NO_3^-$, $SO_4^{2-}$, and $PO_4^{2-}$ are the major accumulated anions. This gave hints about which anions might be substrates for the voltage-dependent anion channel. Indeed, whole-cell patch-clamp recording with various internal anions revealed a high current amplitude for $NO_3^-$ and, unexpectedly, for $SO_4^{2-}$ compared with $Cl^-$. Further experiments using $SO_4^{2-}$, which is usually considered to be an non-permeant anion, provided arguments that this anion not only permeates the channel but also regulates its activity.

[1] This research was supported by the Centre National de la Recherche Scientifique (grant no. UPR0040).

[2] Present address: Department of Biology, University of California at San Diego, 9500 Gilman Drive, La Jolla, CA 92093–0116.

* Corresponding author; e-mail frachisse@isv.cnrs-gif.fr; fax 33–169823768.

## MATERIALS AND METHODS

### Plant Material and Protoplast Isolation

Arabidopsis (ecotype Columbia) seedlings were grown on a medium containing 5 mM $KNO_3$, 2.5 mM $K_2HPO_4$/$KH_2PO_4$, pH 6.0, 2 mM $MgSO_4$, 1 mM $Ca(NO_3)_2$, 1 mM MES, 50 $\mu$M Fe-EDTA, Murashige and Skoog micro-elements (Murashige and Skoog, 1962), 10 g/L Suc, and 7 g/L agar. Culture conditions were 21°C and a 16-h daylength at lighting levels of 120 $\mu$E $m^{-2}$ $s^{-1}$ with neon tubes (a combination of Mazdafluor, Blanc Industrie, Lille, France, and Mazdafluor, Prestiflux, Lille, France). Seedlings aged 7 to 12 d were used for electrophysiological investigations. Hypocotyls were excised from 30 to 40 seedlings, and protoplasts were isolated according to the method of Elzenga (1991) as described in Thomine et al. (1995).

### Electrophysiological Investigations

Patch-clamp experiments were performed as described by Hamill et al. (1981) using a patch-clamp amplifier (EPC 7, List Electronic, Darmstadt, Germany) with a low-pass filter (8-pole Bessel filter) for whole-cell recordings, and an amplifier (model 200A, Axon Instruments, Foster City, CA) for single-channel recordings. During measurements, freshly isolated epidermal protoplasts from Arabidopsis hypocotyls were maintained in bathing medium: 50 mM $CaCl_2$, 5 mM $MgCl_2$, and 10 mM MES-Tris, pH 5.6. The pipettes were filled with 150 mM KCl (or other $K^+$ salts as indicated), 2 mM $MgCl_2$, and 10 mM Tris-HEPES, pH 7.2, supplemented with either 5 mM MgATP and LiGTP or 1 or 3 mM MgATP, as indicated in the figure legends. The free $Ca^{2+}$ concentration of 1 $\mu$M in the pipette, calculated with Ligandy software (Steinhardt Software Bank, Berkeley, CA), was obtained with 5 mM EGTA and 4.2 mM $CaCl_2$. The osmolalities of both solutions were adjusted to 450 mosmol with mannitol using a vapor pressure osmometer (model 5500, Wescor, Logan, UT). Gigaohm resistance seals between pipettes (pipette resistance, 1–5 M$\Omega$) coated with Sylgard (General Electric) pulled from capillaries (Kimax-51, Kimble Glass, Owens, IL) and protoplast membranes were obtained with gentle suction leading to the whole-cell configuration. The liquid junction potentials were measured according to the method of Neher (1992), and all potentials given, including reversal potentials ($E_{rev}$), have been corrected by subtracting the junction potentials for each ionic condition (150 mM $Cl^-$, 2 mV; 150 mM $NO_3^-$, 4 mV; 75 mM $SO_4^{2-}$, 11 mV; 75 mM malate, 19 mV; and 150 mM $HCO_3^-$, 13 mV). Whole-cell currents were measured in response to 10-s voltage ramps from −180 mV to +80 mV. We checked that the estimation of the $E_{rev}$ was independent of the voltage protocol, and similar values were measured using voltage pulse protocols or ramps starting from a positive voltage. We also ensured that, even when we used a two-times faster ramp, the I-V relationship stayed at steady state. To exclude recordings presenting a voltage-independent current, a leak was determined as the linear component between a hyperpolarized potential at which the voltage-dependent current is completely deactivated, and 0 mV, the value at which the leak current is null. The I-V relationships for which the contribution of leak at the peak potential was larger than 30% of the peak current were rejected. Therefore, the permeability ratio has not been corrected.

Outside-out patches were obtained by withdrawing the pipette from the whole-cell configuration. The single-channel recordings were stored on videotape, and digitized with a sample interval of 0.1 ms (five times the filter frequency) using Fetchex (pClamp 6.0.2. Axon Instruments) for analysis. The distribution of amplitudes was fitted by a Gaussian model in pSTAT patch-clamp software (pClamp version 6.0.2., Axon Instruments).

Application of voltage programs and handling of the data were performed using a Digidata 1200 interface (Axon Instruments) and pClamp software with Clampex and Clampfit. The filter frequency was set to 2 kHz, and capacitive transients were corrected during the patch-clamp experiments. The series resistance was compensated to more than 85% when the access resistance was higher than 5 M$\Omega$. Unless otherwise indicated, figures are shown for one representative protoplast, and statistics are given as means ± SE ($n$ indicates the number of protoplasts tested).

Permeability ratios for mixtures of $Cl^-$ and other monovalent anions ($P_{monoval}/P_{Cl}$) or for mixtures of $Cl^-$ and divalent anions ($P_{dival}/P_{Cl}$) were calculated from $E_{rev}$ measurements with Equations 1 and 2, respectively. Both equations were derived from the Goldman-Hodgkin-Katz equation (Lewis, 1979) and adapted to anions.

$$P_{monoval}/P_{Cl} = (Cl_e\, e^{(EF/RT)} - Cl_i)/(A_{i(monoval)}) \quad (1)$$

$$P_{dival}/P_{Cl} = (Cl_e\, e^{(EF/RT)} - Cl_i)(1 + e^{(EF/RT)})/4(A_{i(dival)}) \quad (2)$$

where $E$ is the $E_{rev}$, $R$ is the gas constant, $T$ is the absolute temperature, $F$ is the Faraday's constant, $Cl_e$ and $Cl_i$ are the extracellular and intracellular activities of $Cl^-$, respectively, and $A_{i(monoval)}$ and $A_{i(dival)}$ are the extracellular and intracellular activities of the other intracellular monovalent or divalent anions, respectively. Activity coefficients were estimated according to the method of Dean (1985).

### Anion Content Analysis

Eleven-day-old plantlets grown in vitro on the same medium and in the same conditions as for electrophysiological investigations were harvested. Plants were gathered in pools of five and cut at the level of the crown in order to remove the roots. Each sample (fresh weight around 20 mg) was ground in liquid nitrogen, transferred into an eppendorf tube, suspended in 500 $\mu$L of ultrapure water, and centrifuged for 2 min at 4,000$g$. The supernatant was collected and stored. The pellet was re-extracted three times using the same procedure. The four supernatants of each sample were pooled, filtered on 0.2-$\mu$m sterilized filters (DynaGard, Microgon, Laguna Hills, CA), and used for capillary microelectrophoresis ion determination. The anion concentrations were expressed relative to the plant volume (moles per liter of plant) assuming that the plantlet density is 1 g $mL^{-1}$.

Capillary electrophoresis was performed with an automated analyzer (Quanta 4000, Waters) controlled by a computer fitted with Millenium 2010 software (Waters) running in a Windows environment. Analog data (20-Hz sampling rate) were collected from the column absorbance inverse-UV detector (254 nm). The silica capillary dimensions were 75 $\mu$m i.d. and 60 cm length. The electrolyte solution used for migration was 4.6 mM chromate and 0.5 mM OFM-$Br^-$ at pH 8.0. Separations were performed using a 20-kV applied potential.

## RESULTS

### Anion Selectivity and Permeability of the Voltage-Dependent Anion Channel

We previously identified a channel with a strong voltage-dependence at the plasma membrane of protoplasts from epidermal cells of Arabidopsis hypocotyls. Using $Cl^-$ as the permeant anion, this channel was shown to carry essentially anion currents (Thomine et al., 1995). In the presence of 5 mM intracellular ATP (Thomine et al., 1997a), a voltage ramp from −180 to 80 mV applied at the plasma membrane in the whole-cell configuration allowed us to record an anion current with the characteristic voltage dependence displayed in Figure 1A. For potentials more negative than −130 mV, no current was recorded. Depolarization of the membrane to potentials more positive than −130 mV activated an inward current corresponding to an outward anion flux. For voltages more positive than the peak potential, the current decreased with the diminution of the driving force for anions and reversed as this driving force became in favor of anion influx. The flattening of the curve in the vicinity of the $E_{rev}$ indicated a marked rectification of the current in this voltage range.

To get hints about the possible substrates for plant anion channels, we analyzed the anion content of young plantlets used to prepare hypocotyl protoplasts. The anion content analysis was performed on the aerial part of Arabidopsis seedlings grown and harvested in the same conditions as for patch-clamp experiments. In 11-d-old plantlets, the aerial part consists of a hypocotyl that had already reached its maximum length of about 2 mm, two cotyledons, two fully expanded leaves, and two immature leaves. Ions were separated from aqueous plant extracts by capillary ion electrophoresis (Fig. 2A) as described in "Materials and Methods." Comparison of electrophoregrams of plant ex-

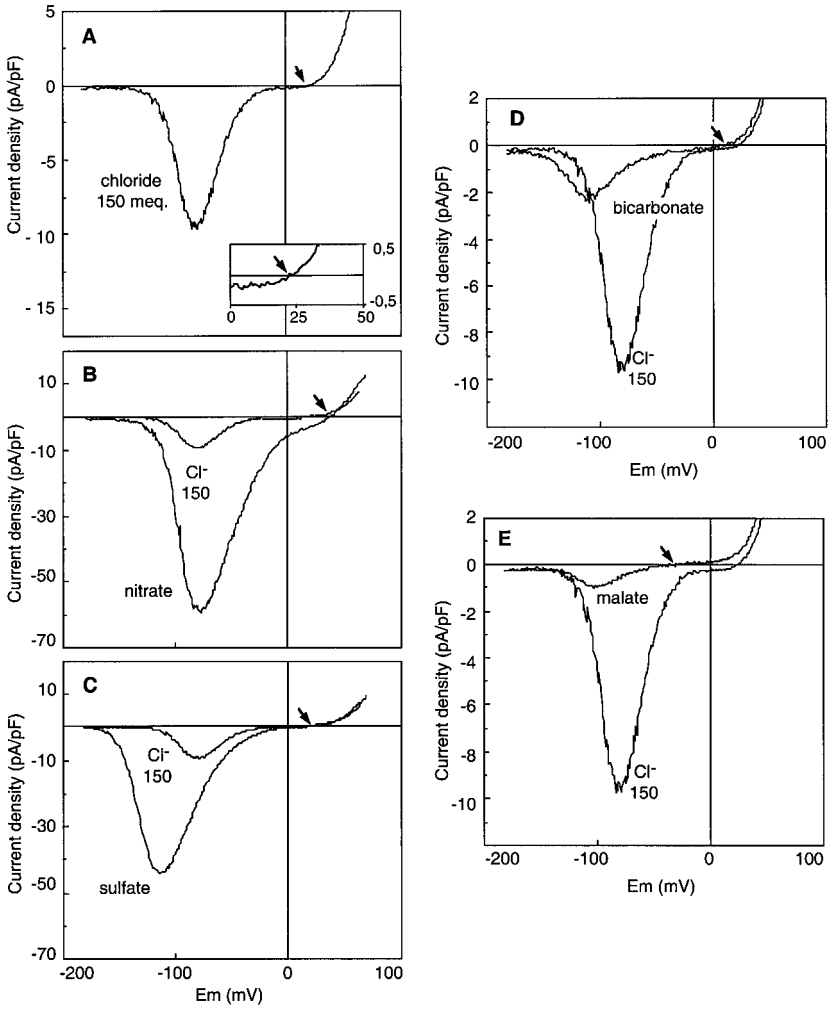


**Figure 1.** Current-voltage relationships of the voltage-dependent anion channel for various intracellular anions. Whole-cell currents were measured on hypocotyl epidermal protoplasts. The currents result from a 10-s voltage ramp from −180 mV to +80 mV applied at the plasma membrane. I-V curves were obtained in the presence of 150 meq $Cl^-$ (A), 150 meq $NO_3^-$ (B), 150 meq $SO_4^{2-}$ (C), 150 meq $HCO_3^-$ (D), or 150 meq malate$^{2-}$ (E). For comparison, each I-V curve is presented with the $Cl^-$ current corresponding to 150 meq $Cl^-$. Note the different current scalings for A and B, C and D, and E. The bath solution contained 110 mM $Cl^-$ and the pipette solution contained 5 mM ATP, 5 mM GTP, 150 meq of the anion to be tested, and 12.4 mM $Cl^-$. Representative I-V curves from data sets of five to 10 independent recordings for each anion are shown, and arrows indicate the position of $E_{rev}$ on the voltage axis. The inset in A shows an expanded picture of the $E_{rev}$ region.

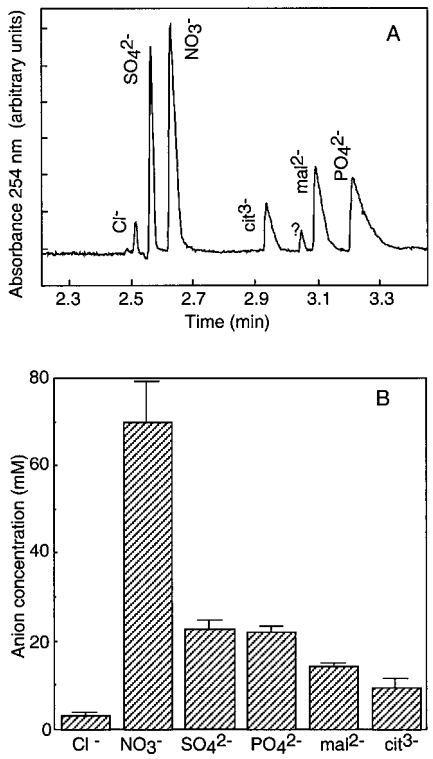


**Figure 2.** Quantitative analysis of the anion content in the aerial parts of 11-d-old Arabidopsis plantlets. A, Capillary ion electropherogram of a water-soluble extract showing the six identified peaks. B, Mean values ± SE of the anion concentrations ($n$ = 9).

tracts and solutions containing reference anions at different concentrations, we identified six peaks corresponding to $Cl^-$, $SO_4^{2-}$, $NO_3^-$, citrate, malate, and $PO_4^{2-}$ (Fig. 2A). The quantification of these peaks (Fig. 2B) revealed a high concentration of $NO_3^-$ (close to 70 mM), a concentration for both $SO_4^{2-}$ and $PO_4^{2-}$ (around 22 mM), and a low concentration for $Cl^-$ (3 mM). For the identified organic anions, malate and citrate, the concentrations were 14.4 and 9.7 mM, respectively.

To determine whether the voltage-dependent channel can allow effluxes of anions other than $Cl^-$, the 150 meq of $Cl^-$ contained in the patch pipette was substituted with 150 meq of $NO_3^-$, $SO_4^{2-}$, malate$^{2-}$, $HCO_3^-$, or Glu provided as $K^+$ salts. The substitution of the cytosolic rather than extracellular anions was favored as closer to the in vivo conditions in which the different anions concentrated inside the cell tend to flow out at physiological membrane potentials, and because it also integrates putative internal regulatory effects of the anions. As previously reported (Thomine et al., 1995), the anion current intensity slowly increased, reached a maximum 3 to 10 min after getting the whole-cell configuration, and started to decrease after a few minutes of steady state. All of the curves presented in the figures and used for the determination of $E_{rev}$ and maximum peak current amplitudes were recorded at the time of maximum activation.

Comparison of the I-V curves in Figure 1 shows a similar voltage dependence for the different channel-mediated anion currents. Some differences appear in the threshold activation potential according to the anion tested; this potential was the most negative for $SO_4^{2-}$ and the least negative for $Cl^-$. Figure 1 reveals large differences in the current amplitude at the peak potential and in the position of the $E_{rev}$ depending on the anion species loaded into the cytosol. The current recorded in the whole-cell configuration reflects the activity of the entire channel population. Two types of information can be deduced from this current. The first one is the current density for each ion tested. The macroscopic whole-cell current ($I$) is the product of the number of functional channels in the cell membrane ($N$), by the open probability of a channel at the peak potential ($P_o$), and the single-channel current ($i$) ($I = iNP_o$). Although the measurement of whole-cell current density combines information about regulatory and permeation properties of an anion toward the channel, it is most likely a physiologically relevant parameter. The second one concerns the selectivity of the channel that can be deduced from the $E_{rev}$. This potential is indicative of the relative affinity of anions for the channel pore, but does not presume the ion permeation through the channel (Hille, 1992).

We compared the whole-cell current at the peak potential for the different intracellular anions (Table I; Fig. 1). The highest current amplitudes were reached when 92% of the intracellular $Cl^-$ was replaced by $NO_3^-$ (Fig. 1B) or $SO_4^{2-}$ (Fig. 1C). Interestingly, small but reproducible currents representing about 25% of the $Cl^-$ current were observed when 92% of the intracellular $Cl^-$ was replaced by $HCO_3^-$ (Fig. 1D). Very low currents with high variability were observed in the presence of malate (Fig. 1E). For these small $HCO_3^-$ and malate currents there was the question of their contamination by inward $Cl^-$ currents corresponding to the 12.4 mM $Cl^-$ left in the pipette solution. Figure 3 shows the peak current amplitudes measured when varying the $Cl^-$ concentration in the pipette (for a total pipette anion content adjusted in each case to 162.4 mM with the non-permeant anion Glu), with $Cl^-$ in the bath kept constant at 110 mM. The intensity of the $Cl^-$ current decreased linearly when $Cl^-$ was replaced by Glu, extrapolating to zero for zero $Cl^-$ in the pipette. This confirmed that Glu could effectively be considered a non-permeant anion. The small current measured with 12.4 mM $Cl^-$ (+150 mM non-permeant Glu) was 1.0 ± 0.2 pA/pF ($n$ = 10), thus representing the contribution of the residual 12.4 mM $Cl^-$ present in all of the pipette solutions. When corrected for this value, the $HCO_3^-$ current appeared 6-fold lower than the $Cl^-$ current. For malate, the high variability of the small corrected current precluded any precise quantitative comparison.

The channel selectivity for each anion was investigated by measuring the $E_{rev}$. The relative permeability ratios for different anions over $Cl^-$ were calculated from the $E_{rev}$ with Equations 1 or 2 (see "Materials and Methods") derived from the Goldman-Hodgkin-Katz current equation. The $E_{rev}$ of the whole-cell current in the presence of 162.4 mM $Cl^-$ in the pipette and 110 mM $Cl^-$ in the bath (20.4 ± 5.6 mV, $n$ = 10) was similar to the calculated equilibrium potential for $Cl^-$ (20.1 mV), indicating that the voltage-dependent inward current is highly selective for anions.

**Table I.** *Peak current amplitudes and permeability ratios for different anions*

Peak current amplitudes and reversal potentials were measured in the whole-cell configuration, with 150 meq $L^{-1}$ of the anion to be tested, 12.4 mM $Cl^-$ in the pipette, and 110 mM $Cl^-$ in the bath. The relative permeability ratios were calculated from Equations 1 and 2 as described in "Materials and Methods." Mean values of peak current and permeability ratios are expressed as ±SE for the number of seals indicated within parentheses.

| | $Cl^-$ ($n$ = 10) | $NO_3^-$ ($n$ = 10) | $SO_4^{2-}$ ($n$ = 7) | $Malate^{2-}$ ($n$ = 5) | $HCO_3^-$ ($n$ = 10) |
|---|---|---|---|---|---|
| $I_{Peak}$ (pA/pF) | −12.0 ± 1.8 | −64.9 ± 9.5 | −67.3 ± 3.4 | −2.0 ± 1.5 | −3.1 ± 0.5 |
| $P_x/P_{Cl}$ | 1.0 ± 0.1 | 2.6 ± 0.3 | 2.0 ± 0.2 | 0.03 ± 0.03 | 0.8 ± 0.1 |

When using a $Cl^-$-free bath solution (CaOH neutralized with MES), no outward current could be detected ($n$ = 5). This shows that in our experimental conditions the outward current is essentially carried by $Cl^-$, excluding any large error in $E_{rev}$ measurement due to an outward $K^+$ current. This was confirmed by showing that the exchange of $K^+$ by $Cs^+$ in the pipette solution did not influence significantly the $E_{rev}$ (40.7 ± 8.5 mV, $n$ = 10 with 150 mM $CsNO_3$, and 41.2 ± 4 mV, $n$ = 10 with 150 mM $KNO_3$). The permeability ratios for a range of physiological anions are reported in Table I. The largest values were obtained for $NO_3^-$ ($PNO_3^-/PCl^-$ =2.6 ± 0.3) and $SO_4^{2-}$ ($PSO_4^{2-}/PCl^-$ =2.0 ± 0.2). The relative permeability of $HCO_3^-$ compared with $Cl^-$ was slightly lower than 1, and malate appeared almost non-permeant. Different ionic conditions were tested to ascertain the relative permeabilities of $NO_3^-$ and $SO_4^{2-}$ over $Cl^-$. For example, a $PNO_3^-/PCl^-$ of 2.9 ± 0.4 ($n$ = 3) was calculated when $NO_3^-$ was added in the bath (100 mM $NO_3^-$ and 10 mM $Cl^-$); the pipette solution contained 150 mM Glu and 12.4 mM $Cl^-$. This value is not significantly different from that obtained in the ionic conditions described in Table I. In summary, these results lead to the following selectivity sequence:

$$NO_3^- \geq SO_4^{2-} > Cl^- > HCO_3^- \gg mal^{2-}$$

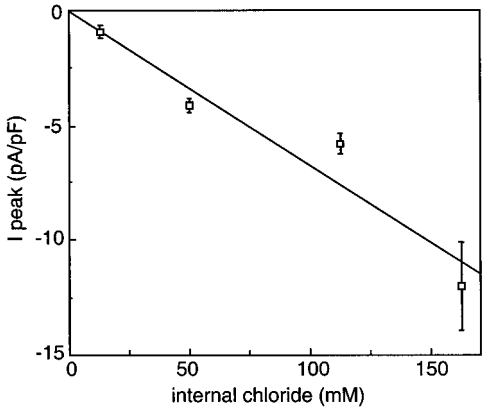


**Figure 3.** Amplitude of the peak current as a function of the internal $Cl^-$ concentration. Internal $Cl^-$ was varied from 12.4 to 162.4 mM while maintaining the total anion concentration in the pipette to 162.4 mM by adding the non-permeant anion Glu. External $Cl^-$ was kept at 110 mM. Peak current amplitudes were measured from 10-s voltage ramps as described in "Materials and Methods." Each current amplitude is the mean ± SE of five to 13 measurements. The line represents the linear regression of the data ($r^2$ = 0.93).

Considering the above results, the most surprising finding was that $SO_4^{2-}$ appears to be a good substrate of the voltage-dependent anion channel. As this anion is usually considered as non-permeant, we performed additional experiments to demonstrate that the current recorded in our experimental conditions of high external $Ca^{2+}$ (50 mM $CaCl_2$) was not a voltage-dependent inward $Ca^{2+}$ current like the one described in carrot cells and Arabidopsis (Thuleau et al., 1994; Thion et al., 1998). Using $SO_4^{2-}$ as the intracellular anion, we applied a voltage ramp every 30 s to monitor the current as a function of time. After getting stable I-V curves for 5 min, we substituted the extracellular solution (50 mM $CaCl_2$ and 5 mM $MgCl_2$) with a $Ca^{2+}$-free solution containing the same amount of $Cl^-$ and a large-spectrum $Ca^{2+}$-channel blocker, $La^{3+}$ (95 mM TEA-Cl and 5 mM $LaCl_3$). Following $Ca^{2+}$ removal, the properties of the current remained unchanged ($n$ = 3; Fig. 4); neither the amplitude nor its $E_{rev}$ was modified. This result rules out the hypothesis that the inward current under investigation bears any significant contribution of $Ca^{2+}$ ions and confirms that it is only carried by $SO_4^{2-}$. Furthermore, the

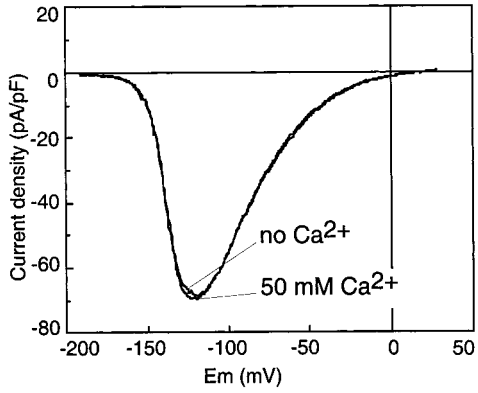


**Figure 4.** Characteristics of the current-voltage relationship in the presence or absence of extracellular $Ca^{2+}$. A 10-s voltage ramp between −180 mV to +30 mV was applied every 30 s. The pipette solution contained: 5 mM ATP, 5 mM GTP, 75 mM $SO_4^{2-}$, and 12.4 mM $Cl^-$. The I-V curve was recorded in the standard bath (50 mM $CaCl_2$ and 5 mM $MgCl_2$) 10 min after breaking to the whole-cell configuration when a stable current amplitude was reached (50 mM $Ca^{2+}$), and after 5 min of perfusion with the $Ca^{2+}$-free bath (no $Ca^{2+}$) (95 mM TEA-Cl, 5 mM $LaCl_3$). Results are shown for one representative experiment out of three. In all cases, the current amplitude was unchanged and the $E_{rev}$ was not significantly modified.

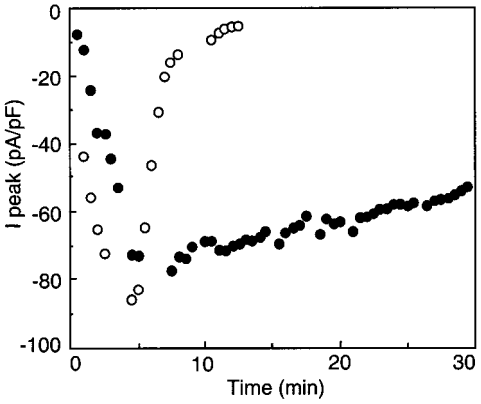


**Figure 5.** Time course of the $NO_3^-$ and $SO_4^{2-}$ currents in the whole-cell configuration. A 10-s voltage ramp between −180 mV to +80 mV was applied every 30 s. The $NO_3^-$ current (○) and the $SO_4^{2-}$ current (●) amplitudes at the peak (I peak) are displayed as a function of time after the establishment of the whole-cell configuration. The pipette solution included either 150 mM $NO_3^-$ or 75 mM $SO_4^{2-}$, 12.4 mM $Cl^-$, and 3 mM ATP, while the bath included 110 mM $Cl^-$. Results are from one representative experiment out of eight for each condition.

nucleotide regulation, a characteristic feature of the $Cl^-$ current mediated by this channel (Thomine et al., 1997a), was also observed with $SO_4^{2-}$ as the intracellular anion (data not shown).

### Regulatory Effects of $SO_4^{2-}$ on the Anion Current

We reported previously (Thomine et al., 1995) that the amplitude of the $Cl^-$ current changed after the establishment of the whole-cell configuration: the amplitude of the current first slowly increased, reached a maximum after 3 to 10 min, and then started to decrease. In all cases, the current completely disappeared within 10 to 30 min. A similar evolution of the current amplitude with time was observed for $NO_3^-$, $HCO_3^-$, and malate. Figure 5 compares the changes of the peak current when either $NO_3^-$ or $SO_4^{2-}$ was used as the internal anion. The $NO_3^-$ current ran down and disappeared completely after 12 min of intracellular perfusion. In contrast, the $SO_4^{2-}$ current decreased very slowly, with the maximal peak current being decreased by about 27% after 30 min. Overall, when a $SO_4^{2-}$-containing solution was perfused through the patch

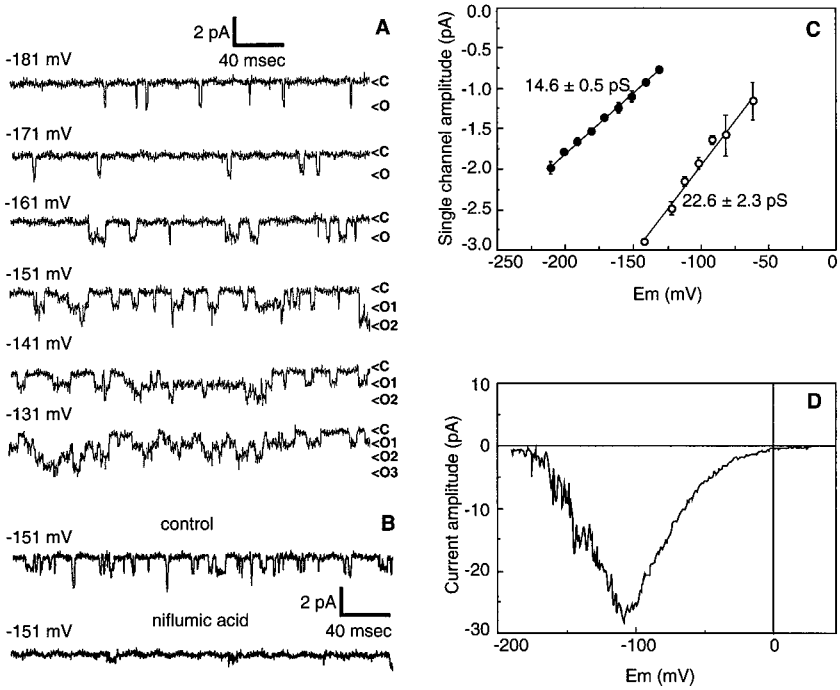


**Figure 6.** $SO_4^{2-}$ permeation through single voltage-dependent anion channels. A, Single-channel currents were recorded in the outside-out configuration with membrane potential clamped in the range −131 mV to −181 mV (c, closed; o, open). The pipette solution included 75 mM $SO_4^{2-}$, 12.4 mM $Cl^-$, and 1 mM ATP, while the bath contained 110 mM $Cl^-$. B, Inhibition of single-channel current by 300 μM niflumic acid. Single-channel currents were recorded in the outside-out configuration with membrane potential clamped at −151 mV. The control trace was obtained 10 s before adding the channel blocker, while the trace in the presence of niflumic acid was obtained about 10 s after adding the blocker. The pipette solution included 75 mM $SO_4^{2-}$, 12.4 mM $Cl^-$, and 3 mM ATP, while the bath was 110 mM $Cl^-$. C, Single-channel I-V curve for $SO_4^{2-}$ current (●) gave a conductance of 14.9 ± 0.5 pS ($n$ = 3). For comparison, channel I-V curve for $Cl^-$ current (○) gave a conductance of 22.6 ± 2.3 pS ($n$ = 3). The pipette solution included either 150 mM $Cl^-$ or 75 mM $SO_4^{2-}$, 12.4 mM $Cl^-$, and 1 mM ATP, while the bath was 110 mM $Cl^-$. D, I-V relationship of an outside-out excised patch that exhibits both the activity of single channels in the range −200 to −100 mV and a typical current rectification in the range −70 to +20 mV, where single channels are not resolved. The pipette solution included 75 mM $SO_4^{2-}$, 12.4 mM $Cl^-$, and 1 mM ATP, while the bath was 110 mM $Cl^-$.

pipette in the whole-cell configuration, the peak current was only decreased by 12% ± 6% after 15 min ($n$ = 8) and by 19% ± 4% after 25 min ($n$ = 4), whereas at this latter time the voltage-dependent current was completely lost with all other anions tested. Thus, $SO_4^{2-}$ is not only a substrate for the voltage-dependent anion channel, it also prevents its run-down. This suggests that $SO_4^{2-}$ ions play a regulatory role on channel activity.

### Single-Channel Analysis of the $SO_4^{2-}$ Current

To analyze further the permeation of $SO_4^{2-}$ ions through the voltage-dependent anion channel of the hypocotyl, we recorded the single-channel activity in the outside-out configuration. Again, in contrast with what happens with $Cl^-$, in the presence of intracellular $SO_4^{2-}$, the anion channel activity did not undergo any run-down. While this allowed us to record channel activity for over 1 h on the same patch, we could never isolate any patch containing less than about five to 10 active channels. This impaired the analysis of channel activity, allowing the single-channel amplitude to be resolved only for potentials more hyperpolarized than −100 mV, at which no more than three to four channel openings overlapped.

Figure 6A illustrates the single-channel activity of the anion channel in the outside-out configuration with an internal solution containing 75 mM $SO_4^{2-}$ and 1 mM ATP. An increase in open probability when the membrane is depolarized was observed (compare −181 mV and −141 mV), which correlated with the voltage dependence of the current in the whole-cell configuration. Niflumic acid, the most potent blocker of the whole-cell anion current (Thomine et al., 1997b), inhibited the single-channel activity (Fig. 6B). The amplitude of single-channel currents was analyzed in the voltage range between −200 mV and −150 mV ($n$ = 3). A linear regression of the I-V plot of single-channel amplitudes yielded a single-channel conductance of 14.6 ± 0.5 picoSiemens (pS) (Fig. 6C). When measured in otherwise identical conditions, the conductance was found to be higher with internal $Cl^-$ (22.6 ± 2.3 pS) than with internal $SO_4^{2-}$ (14.6 ± 0.5 pS) (Fig. 6C). Thus, the 5- to 6-fold increase in $SO_4^{2-}$ whole-cell current compared with $Cl^-$ current could not be accounted for by an increase in single-channel conductance.

A linear extrapolation of the experimental I-V curve obtained with $SO_4^{2-}$ crosses the voltage axis for a value of −78 mV. This value is not in agreement with the $E_{rev}$ value of +16 mV measured in the whole-cell configuration. This difference likely results from current rectification around the $E_{rev}$ occurring at the single-channel level as it occurred at the whole-cell level. Evidence for single-channel current rectification is given by I-V curves from outside-out excised patches containing 20 to 50 channels: they exhibit both the activity of single channels in the range −200 to −100 mV and a typical current rectification in the range −70 to +20 mV, even though single channels cannot be resolved in this range (Fig. 6D).

## DISCUSSION

### Anion Channel Permeability

We investigated the anion selectivity and permeability of the voltage-dependent anion channel of Arabidopsis hypocotyl cells, and analyzed in parallel the anion content of Arabidopsis plantlets by capillary electrophoresis. Such analysis gives only a mean global concentration for each ion species and does not provide information on the localization within plant tissues and cell compartments, but helped us to identify putative substrates for the plasma membrane anion channels.

We found that Arabidopsis anion channels are highly permeable to $NO_3^-$. A large $NO_3^-$ permeability was also found for the two types of anion channels of fava bean guard cells (rapid type: $NO_3^-$ [4.2] > $Cl^-$ [1] ≫ $malate^{2-}$ [0.1], Hedrich and Marten, 1993; slow type: $NO_3^-$ [20.9] > $Cl^-$ [1] ≫ $malate^{2-}$ [0.24], Schmidt and Schroeder, 1994), anion channels from wheat root (Skerrett and Tyerman, 1994), cotyledonary cells of amaranth ($NO_3^-$ [2.4] > $Cl^-$ [1], Terry et al.,1991), pea epidermal cells ($NO_3^-$ [1.34] > $Cl^-$ [1] ≫ $malate^{2-}$ [0.002], Elzenga and Van Volkenburgh, 1994), and suspension-cultured coffee cells (Dieudonné et al., 1997). High $NO_3^-$ permeability thus seems to be a general feature of plant plasma membrane anion channels. The finding that $SO_4^{2-}$, which is usually considered to be a weakly permeant or non-permeant ion in anion channels, was indeed permeant in the Arabidopsis voltage-dependent anion channel is a striking and novel result from this study. Although the $SO_4^{2-}$ uptake transporter of the plasma membrane has been extensively studied (Rennenberg et al., 1989; Clarkson et al., 1992), we report here the first example (to our knowledge) of large channel-mediated $SO_4^{2-}$ currents.

Phosphate permeability has not been investigated because $Ca^{2+}$ phosphate precipitation is a technical limitation that we have not yet been able to overcome. Malate is only weakly permeant through the Arabidopsis hypocotyl anion channel, as already shown for the rapid and slow anion channels in guard cells (Hedrich and Marten, 1993; Schmidt and Schroeder, 1994). Glu, with the highest $M_r$ of the anions tested, is not significantly permeant and can thus be safely used as a reference nonpermeating anion. Our data showing small but reproducible $HCO_3^-$ currents open an interesting new area of investigations. $HCO_3^-$ permeability of plant anion channels has, to our knowledge, never been reported, and even information concerning the permeability of animal channels to $HCO_3^-$ is scarce. However, $HCO_3^-$ permeability can be quite significant, as exemplified by the anion channel of human secreting epithelia, for which a $HCO_3^-$ permeability ratio $PHCO_3^-$ to $PCl^-$ in the range of 0.50 to 0.64 has been reported (Tabcharani et al., 1989) and by the cystic fibrosis transmembrane conductance regulator for which a $PHCO_3^-$ to $PCl^-$ ratio of 0.14 to 0.25 has been recently measured (Linsdell et al., 1997). Several technical difficulties, among which the small amplitude of the currents and the run-down of the channel, limit the study of the $HCO_3^-$ currents mediated by the voltage-dependent anion channel

of Arabidopsis hypocotyls. Nevertheless, the potential roles of channel-mediated $HCO_3^-$ fluxes in pH regulation and/or carbon metabolism call for such a study to be undertaken.

The high $NO_3^-$ and $SO_4^{2-}$ whole-cell currents mediated by the voltage-dependent anion channel of Arabidopsis hypocotyls, combined with the high concentrations of $NO_3^-$ and $SO_4^{2-}$ in plantlet tissues, suggest that these two ions are in vivo substrates of the channel and that the channel could play a role in the homeostasis of their cellular concentrations.

### $SO_4^{2-}$ Regulation of the Anion Channel

In addition to its unusual permeation, the second property of $SO_4^{2-}$ is its regulatory effect on the channel. As measured on excised outside-out patches, the anion channel conductance was higher in the presence of internal $Cl^-$ compared with $SO_4^{2-}$. This can be reconciled with the results of whole-cell $E_{rev}$ measurements. These $E_{rev}$ values indicate that $SO_4^{2-}$ has a higher affinity for the channel pore than $Cl^-$. As $SO_4^{2-}$ is more tightly bound inside the channel, it tends to reside longer in the channel pore, which results in a lower rate of permeation (as revealed by lower single-channel conductance). However, the high whole-cell current density cannot be accounted for by a higher permeation rate, since the single-channel conductance is actually lower. This indicates that $SO_4^{2-}$ modifies other parameters that determine the whole-cell current density: the open probability ($P_o$) or the number of active channels ($N$).

From the single-channel amplitude of the $SO_4^{2-}$ current at the peak potential (Fig. 6C) and the mean whole-cell current density at the same potential (Fig. 1C), we estimated at least 4,000 to 6,000 active channels for a cell 40 $\mu$m in diameter. A number of active channels about 10-fold lower was estimated to account for whole-cell $Cl^-$ currents. These estimations suggest that the large amplitude of the whole-cell $SO_4^{2-}$ currents compared with the $Cl^-$ currents results not only from the more hyperpolarized activation potential (see Fig. 1) but also from a regulatory effect of $SO_4^{2-}$ on the number of active channels. Another effect of $SO_4^{2-}$ was to prevent the run-down of the anion current both in the whole-cell and in the outside-out configuration. Thus, $SO_4^{2-}$ is able to maintain the channel in an active state. This effect was initially observed when this anion was used as the major substrate for the anion channel, i.e. with 75 mM internal $SO_4^{2-}$. No dose response of the regulatory effect of $SO_4^{2-}$ has been constructed, but when the $SO_4^{2-}$ solution was diluted in the $Cl^-$ solution to one-half (75 mM Cl and 37.5 mM $SO_4^{2-}$), one-fourth (112.5 mM Cl and 18.8 mM $SO_4^{2-}$), and one-sixteenth (131.3 mM Cl and 9.4 mM $SO_4^{2-}$), the run-down remained slower than in the presence of $Cl^-$ only (data not shown). The fact that $SO_4^{2-}$ was also able to prevent run-down in excised patches suggests either a direct action on the channel or a membrane-delimited activation pathway. The mechanism underlying the regulatory effect of $SO_4^{2-}$ is still unknown, but it appears to be quite different from other types of run-down prevented by effectors of tubulin (Thion et al., 1996, 1998), indicating the involvement of the cytoskeleton, or by effectors of protein kinase or phosphatase (Wang et al., 1991), indicating a regulation via phosphorylation. The stabilizing effect of $SO_4^{2-}$ suggests an original mechanism that could involve a regulatory site where most anions except $SO_4^{2-}$ bind and induce run-down or where only $SO_4^{2-}$ can bind to prevent run-down. Understanding this mechanism will require further investigation.

### A Metabolic Link between $NO_3^-$ and $SO_4^{2-}$ Permeation and the Regulation of the Channel by Nucleotides?

Considering together the high $NO_3^-$ and $SO_4^{2-}$ whole-cell currents mediated by the channel and the channel regulation by nucleotides raises the hypothesis that this channel could function as a metabolic valve to avoid the cytoplasmic accumulation of $NO_3^-$ and $SO_4^{2-}$ ions when they cannot be extensively metabolized. $SO_4^{2-}$ assimilation requires an ATP-sulfurylase whose activity is directly controlled by the ATP status (Schmidt and Jäger, 1992), while $NO_3^-$ reduction and incorporation into amino acids is a highly energy-consuming process (Botrel and Kaiser, 1997). The voltage-dependent anion channel could be involved in the regulation of the cytosolic concentration of $NO_3^-$ and $SO_4^{2-}$, depending on the variation of the energy balance of the cell. When the energy level of the cell is high, which is reflected by an increased cytosolic ATP concentration, the efflux channel is inhibited (Thomine et al., 1997a), $NO_3^-$ and $SO_4^{2-}$ are trapped in the cytoplasm, where they can be reduced and incorporated into amino acids. Alternatively, when the energy level of the cell is decreased, the ATP and ADP concentrations are reduced and the channel is not inhibited, allowing the efflux of these anions out of the cytoplasm, where no energy for their metabolism is available.

In conclusion, the voltage-dependent anion channel of Arabidopsis hypocotyl cells shares a high permeability to $NO_3^-$ with the previously described plant anion channels. It exhibits a first original property of being permeable to $SO_4^{2-}$ with a unitary conductance about two-thirds that of $Cl^-$. The second original property concerns the strong regulatory effect of $SO_4^{2-}$, increasing the number of active channels per cell and responsible for the large whole-cell $SO_4^{2-}$ currents measured. These properties associated with high concentrations of $NO_3^-$ and $SO_4^{2-}$ in Arabidopsis plantlets highlight the likely participation of the voltage-dependent channel in in vivo $NO_3^-$ and $SO_4^{2-}$ fluxes through the plasma membrane contributing to the homeostasis of their cellular concentrations and metabolism.

Received January 4, 1999; accepted June 8, 1999.

### LITERATURE CITED

**Botrel A, Kaiser WM** (1997) Nitrate reductase activation state in barley roots in relation to the energy and carbohydrate status. Planta **201:** 496–501

**Cho MH, Spalding EP** (1996) An anion channel in *Arabidopsis* hypocotyls activated by blue light. Proc Natl Acad Sci USA **93:** 8134–8138

**Clarkson DT, Hawkesford MJ, Davidian JC, Grignon C** (1992) Contrasting responses of sulfate and phosphate transport in barley (*Hordeum vulgare* L.) roots to protein-modifying reagents and inhibition of protein synthesis. Planta **187:** 306–314

**Dean JA** (1985) Lange's Handbook of Chemistry, Ed 13. McGraw-Hill, New York

**Dieudonné S, Forero ME, Llano I** (1997) Two different conductances contribute to the anion current in *Coffea arabica* protoplasta. J Membr Biol **159:** 83–94

**Ebel J, Cosio EG** (1994) Elicitors of plant defense responses. Int Rev Cytol **148:** 1–36

**Elzenga JTM** (1991) Patch clamping protoplasts from vascular plants. Plant Physiol **97:** 1573–1575

**Elzenga JTM, Van-Volkenburgh E** (1994) Characterization of ion channels in the plasma membrane of epidermal cells of expanding pea (*Pisum sativum* arg.) leaves. J Membr Biol **137:** 227–235

**Hamill OP, Marty A, Neher E, Sakmann B, Sigworth FJ** (1981) Improved patch-clamp techniques for high-resolution current recording from cells and cell-free membrane patches. Pflügers Arch **391:** 85–100

**Hedrich R, Marten I** (1993) Malate induced feedback regulation of plasma membrane anion channels could provide a $CO_2$ sensor to guard cells. EMBO J **12:** 897–901

**Hille B** (1992) Ionic Channels of Excitable Membranes, Ed 2. Sinauer Associated, Sunderland, MA

**Jabs T, Tschöpe M, Colling C, Hahlbrock K, Scheel D** (1997) Elicitor-stimulated ion fluxes and $O^{2-}$ from the oxidative burst are essential components in triggering defense gene activation and phytoalexin synthesis in parsley. Proc Natl Acad Sci USA **94:** 4800–4805

**Lewis CA** (1979) Ion-concentration dependence of the reversal potential and the single channel conductance of ion channels at the frog muscular junction. J Physiol **286:** 417–445

**Linsdell P, Tabcharani JA, Rommens JM, Hou Y-X, Chang X-B, Tsui L-C, Riordan JR, Hanrahan JW** (1997) Permeability of wild-type and mutant cystic fibrosis transmembrane regulator chloride channels to polyatomic anions. J Gen Physiol **110:** 355–364

**Murashige T, Skoog F** (1962) A revised medium for rapid growth and bioassays with tobacco tissue cultures. Physiol Plant **15:** 473–497

**Neher E** (1992) Correction for liquid junction potentials in patch-clamp experiments. Methods Enzymol **207:** 123–131

**Rennenberg H, Kemper O, Thoene B** (1989) Recovery of sulphate transport into heterotrophic tobacco cells from inhibition by reduced glutathione. Physiol Plant **76:** 271–276

**Schmidt A, Jäger K** (1992) Open questions about sulfur metabolism in plant. Annu Rev Plant Physiol Plant Mol Biol **43:** 325–349

**Schmidt C, Schroeder JI** (1994) Anion selectivity of slow anion channels in the plasma membrane of guard cells. Plant Physiol **106:** 383–391

**Skerrett M, Tyerman SD** (1994) A channel that allows inwardly directed fluxes of anions in protoplasts derived from wheat roots. Planta **192:** 295–305

**Tabcharani JA, Jensen TJ, Riordan JR, Hanrahan JW** (1989) Bicarbonate permeability of the outwardly rectifying anion channel. J Membr Biol **112:** 109–122

**Terry BR, Tyerman SD, Findlay GP** (1991) Ion channels in the plasma membrane of *Amaranthus* protoplasts: one cation and one anion channel dominate the conductance J Membr Biol **121:** 223–236

**Thion L, Mazars C, Nacry P, Bouchez D, Moreau M, Ranjeva R, Thuleau P** (1998) Plasma membrane depolarization-activated calcium channels, stimulated by microtubule-depolymerizing drugs in wild-type *Arabidopsis thaliana* protoplasts, display constitutively large activities and a longer half-life in *ton* 2 mutant cells affected in the organization of cortical microtubules. Plant J **13:** 603–610

**Thion L, Mazars C, Thuleau P, Graziana A, Rossignol M, Moreau M, Ranjeva R** (1996) Activation of plasma membrane voltage-dependent calcium-permeable channels by disruption of microtubules in carrot cells. FEBS Let **393:** 13–18

**Thomine S, Guern J, Barbier-Brygoo H** (1997a) Voltage-dependent anion channel of Arabidopsis hypocotyls: nucleotide regulation and pharmacological properties. J Membr Biol **159:** 71–82

**Thomine S, Lelièvre F, Boufflet M, Guern J, Barbier-Brygoo H** (1997b) Anion channel blockers interfere with auxin responses in dark-grown Arabidopsis hypocotyls. Plant Physiol **115:** 533–542

**Thomine S, Zimmermann S, Guern J, Barbier-Brygoo H** (1995) ATP-dependent regulation of an anion channel at the plasma membrane of epidermal cells of Arabidopsis hypocotyls. Plant Cell **7:** 2091–2100

**Thuleau P, Ward JM, Ranjeva R, Schroeder JI** (1994) Voltage-dependent calcium-permeable channel in the plasma membrane of higher plant cell. EMBO J **13:** 2970–2975

**Wang L-M, Salter MW, MacDonald JF** (1991) Regulation of kainate receptors by cAMP-dependent protein kinase and phosphatase. Science **253:** 1132–1134

**Ward JM, Pei Z-M, Schroeder JI** (1995) Role of ion channels in initiation of signal transduction in higher plants. Plant Cell **7:** 833–844